Title

Systematic array processing of a decade of global IMS infrasound data

Authors
Ceranna, L
Matoza, Robin
Hupe, P
et al.

Publication Date
2023-12-14

Chapter 13
Systematic Array Processing of a Decade of Global IMS Infrasound Data

Lars Ceranna, Robin Matoza, Patrick Hupe, Alexis Le Pichon and Matthieu Landès

Abstract The ability of the International Monitoring System (IMS) global infrasound network to detect atmospheric explosions and other events of interest depends strongly on station-specific ambient incoherent noise and clutter (real but unwanted infrasound waves, coherent on an infrasound array). Characterization of coherent infrasound is important for quantifying the recording environment at each station and for assessing the detection probability of specific signals of interest. We systematically characterize coherent infrasound recorded by the IMS network over 10 years on 41 stations over a broad frequency range (0.01–5 Hz). This multiyear processing emphasizes continuous signals such as mountain associated waves and microbaroms, as well as persistent transient signals such as repetitive volcanic, surf, thunder, or anthropogenic activity. We estimate the primary source regions of continuous coherent infrasound using a global cross-bearings approach. For most IMS arrays, the detection of persistent sources is controlled by the dynamics of the stratospheric wind circulation from daily to seasonal scales. Systematic and continuous characterization of multiyear array detections helps to refine knowledge of the source of ambient ocean noise and provides additional constraints on the dynamics of the middle atmosphere where data coverage is sparse.

L. Ceranna (✉) · P. Hupe
BGR, B4.3, 30655 Hannover, Germany
e-mail: lars.ceranna@bgr.de

R. Matoza
Department of Earth Science and Earth Research Institute,
University of California, Santa Barbara, CA 93106-9630, USA

A. Le Pichon
CEA, DAM, DIF, F-91297 Arpajon, France

M. Landès
European-Mediterranean Seismological Centre C/O, CEA, DAM, DIF,
F-91297 Arpajon, France

A. Le Pichon et al. (eds.), *Infrasound Monitoring for Atmospheric Studies*,
https://doi.org/10.1007/978-3-319-75140-5_13

13.1 Introduction

The global International Monitoring System (IMS) infrasound network was designed to reliably detect a one kiloton equivalent explosion worldwide with at least two stations and thus to monitor compliance with the Comprehensive Nuclear Test-Ban Treaty (CTBT) (Christie and Campus 2010). Although the 60-station network is not yet fully established, 49 certified stations now provide global coverage of geophysical and anthropogenic events (Campus and Christie 2010; Marty et al. 2019; Mialle et al. 2019). In addition to its primary function of detecting explosions, the IMS network has demonstrated its potential application in monitoring natural hazards such as large volcanic explosions (Matoza et al. 2019) and severe weather (Waxler and Assink 2019).

The performance of the IMS network is a key concern for the CTBT as environmental noise and coherent clutter may interfere with the detection and identification of explosive events, so their understanding and characterization is important for treaty verification. The detection capability of the infrasound network exhibits significant spatiotemporal variation, which is in part controlled by the station-specific ambient recording environment, which includes incoherent wind noise and persistent unwanted real coherent infrasonic signals (clutter). Clutter can interfere with the detection or successful identification of signals of interest by effectively obscuring or overwhelming a range of look directions (at a given frequency) at a given station. Variations in clutter result from changes in both the source distribution (e.g., Landès et al. 2012) and the propagation conditions (e.g., Evers and Siegmund 2009; Assink et al. 2014), and can be characterized statistically.

IMS infrasound array data are routinely processed at the International Data Center (IDC). The wave parameters of the detected signals are estimated with the Progressive Multi-Channel Correlation method (PMCC) (Cansi 1995). This method proved to be very efficient for routine identification of low-amplitude coherent waves within incoherent noise (Mialle et al. 2019). The initial implementation of PMCC used a series of linearly spaced frequency bands, which in practice (due to computational limitation) had the disadvantage of requiring multiple independent runs to cover the broad frequency band of interest (~0.01–5 Hz). A practical benefit was subsequently gained by implementing PMCC with a variable window length and log-spaced frequency bands (Brachet et al. 2010; Le Pichon et al. 2010), which allows the full frequency range of interest to be processed efficiently in a single computational run. Using this implementation, a first global and multiyear systematic broadband (0.01–5 Hz) analysis of historical IMS records was carried out by Matoza et al. (2013). Matoza et al. (2013) made relative comparisons of the IMS stations' ambient coherent infrasound amplitudes and overall station performance characteristics from April 1, 2005 to December 31, 2010.

In this chapter, we extend our processing of the IMS continuous waveform archive to January 1, 2015, representing almost a decade of IMS waveform data considered. In Sect. 13.2, we introduce the dataset and describe the array processing scheme. In Sect. 13.3, we present the multiyear and global processing results. One dominant factor influencing infrasound detection at mid-latitudes is the spatiotemporal variability of the stratospheric waveguide structure. In particular, the seasonal reversal of the stratospheric circulation oscillation, clearly captured in climatological wind models, controls to first order where signals are expected to be detected (e.g., Drob et al. 2003; Drob 2019). Our processing results provide useful insight into the evaluation of the overall performance of the IMS network. In the last section, we apply a cross-bearing approach proposed by Landès et al. (2012) to reconstruct the main source regions of microbaroms and mountain associated waves (MAW), which dominate the background wavefield. The seasonal patterns of the microbarom source regions are compared with those predicted by nonlinear ocean wave interaction models (Longuet-Higgins 1950; Waxler and Gilbert 2006; Ardhuin and Herbers 2013). We address the implications of our results for the treaty verification which, compared to previous studies, provide progress toward an improved characterization of the space-, time-, and frequency-dependent coherent noise. Moreover, such knowledge is of importance for the development of atmospheric remote sensing methods as useful integrated information about the vertical structure of the temperature and wind are reflected in continuous signals from natural sources (e.g., Le Pichon et al. 2015; Assink et al. 2019; Chunchuzov and Kulichkov 2019; Smets et al. 2019).

13.2 Data and Methods

We perform broadband array processing with the IMS continuous waveform archive of 41 certified stations from April 1, 2005 to January 1, 2015 (Fig. 13.1, left). Each station consists of an array of at least four sensors with a flat response from 0.01 to 8 Hz. Since the IMS network is currently under construction, data availability varies throughout the time period considered. Stations recently installed are not considered in this study due to limited data availability. We restrict our analysis to stations for which there are at least 5 years of continuous recordings available. For 35 stations, data are available for more than 9 years. The spatial distribution of these sites covers a wide range of latitudes, atmospheric, and oceanic conditions (e.g., island, coastal, or interior continental stations). All infrasound stations are composed of four or more microbarometers and include spatial wind-filtering systems and communication facilities (Marty 2019).

Data are processed automatically using the Progressive Multi-Channel Correlation (PMCC) algorithm (Cansi 1995; Mialle et al. 2019). PMCC estimates the wavefront parameters (e.g., back azimuth, apparent velocity, frequency, root mean

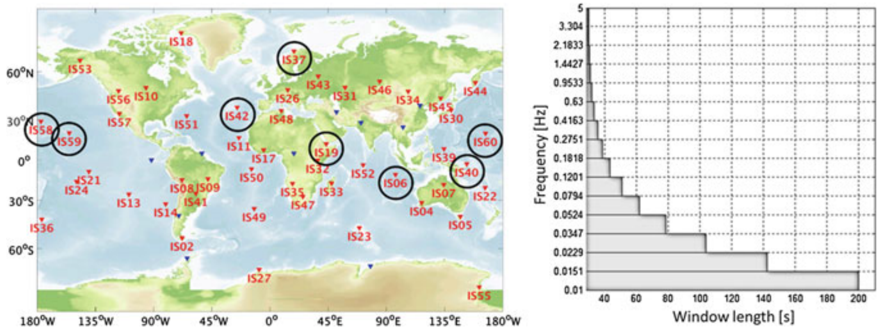

Fig. 13.1 Left: among the 48 certified IMS infrasound stations (red inverted triangles); stations with less than 5 years of archived data are not considered in this study (circled). Right: PMCC configuration using 15 log-scaled frequency bandwidths with window length linearly scaled to the period

square amplitude) of coherent plane waves in a given time window and band-pass filter from the time delays calculated between pairs of sensors. To minimize errors in the calculation of the wave parameters, distant sensors are progressively added. The progressive use of distant sensors has two main effects: the removal of false detections due to correlated noise at the scale of the starting sub-arrays, and a better estimation of the wavefront parameters by increasing the array aperture. The processing is performed over successive overlapping time windows and adjacent frequency bands covering the whole period of analysis. We implement a configuration of 15 bands spaced logarithmically between 0.01 and 5 Hz, with window lengths varying linearly with the period (Fig. 13.1, right). This configuration is a step toward practical improvement of infrasound detection algorithm to better discriminate between interfering signals by defining standard frequency bands for use in the infrasound research community (Garcés 2013).

The resulting detections can be broadly interpreted and classified into three main frequency bands:

- above 0.5 Hz, detections (~30%) are transient signals of natural or man-made origin (e.g., volcanoes, surf, industrial activity) propagating over distances of several hundred kilometers;
- between 0.1 and 0.5 Hz, detections (~60%) are dominated by microbarom signals and remote large events such as explosions, meteorites, and volcanoes (e.g., Campus and Christie 2010; Green et al. 2010; Silber et al. 2019; Matoza et al. 2019);
- below 0.1 Hz, detections (~10%) are associated with large-scale atmospheric disturbances such as MAW generated by tropospheric wind flow over high mountain ranges and, at high latitudes, geomagnetic and auroral activity (Wilson et al. 2010).

13.3 Global Infrasonic Detection and Middle Atmospheric Dynamics

Figure 13.2 summarizes results from the continuous processing for the decade 2005–2015. In the 0.1–0.5 Hz band, the dominant source is microbaroms caused by the nonlinear interaction of oceanic waves, near-continuously detected worldwide (e.g., Garcés et al. 2004; Waxler and Guilbert 2006; Landès et al. 2012). In the northern hemisphere, signals mainly originate from ocean swells in the Pacific, Atlantic, and Indian oceans. For austral IMS stations, the main sources of signals are large swell systems driven by strong continuous eastward surface winds along the Antarctic Circumpolar Current (ACC) which links the major southern oceans in the 50–60°S range (e.g., Landès et al. 2014).

The effective sound speed ratio (V_{RATIO}) defined here by the ratio between the effective sound speed at 50 km altitude and the sound speed at the ground level is

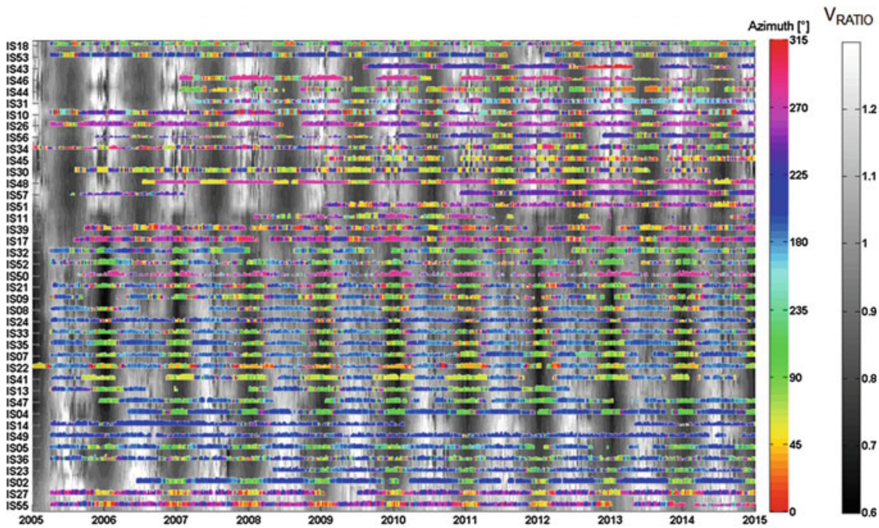

Fig. 13.2 Summary of a decade of IMS infrasound detections in the 0.01–5 Hz frequency band. The 41 IMS stations analyzed are sorted by latitude. Colored rectangles represent the number of detections (each rectangle is one week, height log-scaled with an upper limit of 2800 detections). Colors refer to the weekly averaged back azimuths. At each station, the detections (colored rectangles) are superimposed on V_{RATIO} at 50 km altitude (grayscale). The temperature and wind profiles are extracted using the ECMWF operational analyses part of the Integrated Forecast System (IFS) (91 vertical levels up to 0.01 hPa with a horizontal resolution of half a degree and a temporal resolution of 6 h). Light and dark colors indicate up- and downwind eastward propagation scenarios, respectively. As a result of the seasonal zonal wind reversals in the stratosphere, clear seasonal variations in back azimuths are observed. In the northern hemisphere summer (from June to August), signals from easterly directions dominate and vice versa during winter (from November to January). An opposite trend is noted in the southern hemisphere

superimposed on the detections. This dimensionless parameter represents the combined effects of refraction due to a sound speed gradient and advection due to along-path wind on infrasound propagation (e.g., Green et al. 2012) using the High Resolution (HRES) European Centre for Medium-Range Weather Forecasts models (ECMWF, http://www.ecmwf.int/). The observed azimuthal seasonal trend correlates well with the variation of V_{RATIO}. A clear seasonal transition in the bearings is observed correlated with changes in the stratospheric general circulation between summer and winter. Our global analysis indicates that the primary factor controlling the signal detectability is the seasonal reversal of the prevailing zonal wind at mid-latitudes, anticorrelated from the southern and northern hemispheres, since ~80% of the detections in the 0.2–2 Hz bandpass are associated with propagation downwind of the dominant stratospheric wind direction. This oscillation controls to first order where infrasound detections are predicted.

13.4 Locating the Main Source Regions of Continuous Coherent Ambient Noise

Modern seismological and infrasound networks produce large quantities of continuous waveform data that are dominated by background noise which has strong amplitudes near 0.15–0.2 Hz. The large amplitudes of background seismic and atmospheric waves, secondary microseisms and microbaroms, are generated by the interaction of ocean gravity waves with the seafloor and the atmosphere, respectively caused by the nonlinear interference of oceanic waves with the same frequency propagating in opposite directions (Longuet-Higgins 1950). Microbarom generation is directly proportional to oceanic wave interaction (e.g., Waxler and Gilbert 2006). Using the 2005–2015 broadband reprocessing results of the global IMS archive, the main source regions of continuous coherent signals can be estimated. Following the approach proposed by Landès et al. (2012), a monthly averaged spatial source distribution of microbaroms is estimated. The reconstructed regions are compared with those predicted by the theory of noise generation in the solid Earth, oceans, and atmosphere developed by Ardhuin and Herbers (2013) as an alternative to the Green's function formalism proposed by Waxler and Gilbert (2006). The microbarom source model used, valid in deep water, includes nonlinear ocean wave interaction induced by coastal reflections. Applied to acoustic waves in the atmosphere, it extends previous theories that were limited to vertical propagation only.

Figure 13.3 compares the reconstructed and modeled microbarom source regions for January, April, July, and October averaged over the 2005–2015 period. The observed and predicted source regions both exhibit a clear seasonal variability. The source amplitude and number of microbarom signals are larger in local winter than in summer. In the northern hemisphere, signals mainly originate from storms

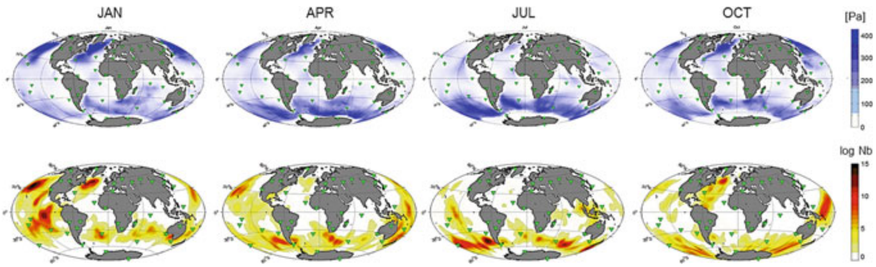

Fig. 13.3 Comparisons between the averaged reconstructed and modeled microbarom source regions for January, April, July and October over the 2005–2015 period. Top: predicted source pressure (in Pa) at the ocean–atmosphere interface highlighting regions of nonlinear interaction of oceanic waves (Ardhuin and Herbers 2013). Bottom: microbarom source regions reconstructed from the broadband reprocessing results using the cross-bearing approach developed by Landès et al. (2012); the colorbar codes the number of intersected back azimuths in a logarithm scale

traveling in opposite direction in the Pacific, Atlantic, and Indian oceans. For austral stations, signals originate from large swell systems driven by strong eastward surface winds along the ACC. Such observations are consistent with the characterization of microseismic noise recorded by worldwide distributed seismic stations (e.g., Stehly et al. 2006; Schimmel et al. 2011). In particular, Schimmel et al. (2011) showed that continental stations can record microseisms generated several thousands of kilometers away and reported similar seasonal variability and latitudinal dependence of the power of secondary microseisms.

We apply the same cross-bearing procedure to the assumed MAW signals with periods selected between 20 and 50 s. Figure 13.4 presents the averaged location results in January, April, July, and October. Hotspots of sources, inferred to be MAW, are found in local winter over the Himalayas, the Rocky and Andes Mountains in America (Le Pichon et al. 2010). Some activity is found over New Zealand where the chain of the Southern Alps culminates at 3700 m. Earlier work published by Larson et al. (1971) pointed out similar features for MAW traveling at acoustic velocities in the 10–100 s period range. Statistical analyses of long-duration atmospheric waves, lasting for several hours to several days were carried out. Using several infrasound observatories in North America, triangulation showed the principal source areas to be along the coast of British Columbia and in the inland Rocky Mountains of the British Columbia-Alberta border. Statistical analyses of MAW characteristics together with general wind circulation patterns were examined. Clear correlation between the amplitude MAW and the annual variation of both zonal and kinetic energy of tropospheric winds in the layer 850–500 hPa (altitude from about 1500–5500 m) was found. The production of infrasound by several possible aerodynamic processes has been examined (e.g., Chunchuzov 1993). The main source mechanism involved at the origin of MAW is explained by stably stratified air passing over a mountain barrier which produces an oscillatory motion of the fluid by interaction with the obstacle. Their impact on the

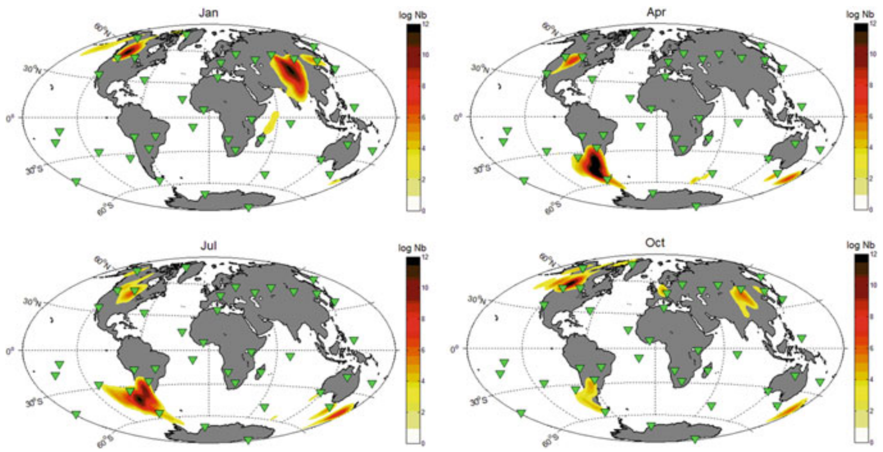

Fig. 13.4 Averaged reconstructed source regions of MAW for January, April, July, and October over the 2005–2015 period. The colorbar codes the number of intersected back azimuths of detections with periods ranging between 20 and 50 s in a logarithm scale

dynamics of the middle atmosphere has been demonstrated. Theoretical and experimental diagnostic tools to further investigate the upward propagation of the transferred energy flux of mountain waves through the lower stratosphere have been investigated (e.g., Smith et al. 2007).

13.5 Discussion and Conclusions

Reprocessing a 10-year archive of continuous waveform data from the IMS infrasound network in the 0.01–5 Hz band permits statistical characterization and analysis of the coherent ambient wavefield in the frequency band relevant to explosion monitoring. We implemented a standardized PMCC configuration between 0.01 and 5 Hz which consists of 15 log-spaced frequency bands and window lengths varying linearly with the period. This configuration allows computationally efficient broadband processing and helps with signal discrimination. It provides progress toward more accurate metrics to evaluate the detection capability of the IMS infrasound network (Marty 2019). Since the ambient noise limits the ability to detect and identify signals of interest, incorporating realistic station-, time-, and frequency-dependent coherent noise levels can improve detection capability estimates (Le Pichon et al. 2012; Green and Bowers 2010).

Comparison with the dynamical features of global atmospheric circulation highlights the strong influence of the spatiotemporal variability of the stratospheric waveguide structure on the network detection capability. Among the natural sources of infrasound dominating the coherent background noise are long lasting signals such as microbaroms and MAW observed at most middle- and high-latitude stations. The reconstructed and predicted microbarom source regions using two-dimensional wave energy spectrum ocean wave products are in good agreement. Dominant regions are found thousands of kilometers away from the IMS stations and exhibit clear seasonal variability in amplitude and latitudinal dependence. Combining infrasound and microseism observations from long running stations would be beneficial to further assess numerical models of noise generation in the solid Earth, oceans, and atmosphere and characterize inter-decadal climate change (Schimmel et al. 2011). In the 10–100 s period range, MAW are continuously and globally detected. Triangulation using MAW observations at several stations shows prominent source energy over high mountain ranges in local winter. Climatological statistics of their characteristics can provide useful quantitative measures of orographic convective instabilities and improve the parameterization of gravity waves due to sub-grid-scale orography for Numerical Weather Prediction (NWP) applications (e.g., McFarlane 1987; Kim and Arakawa 1993).

Observations from natural sources detected worldwide are of great interest for the application of infrasound as a passive remote sensing technique of the upper atmosphere (Assink et al. 2014), for which there is renewed interest. Following the pioneering studies of Donn (1973) and Larson et al. (1971), the recent advances in measurement, processing methods, and modeling techniques provide new insights on method for continuous, passive acoustic tomography of the atmosphere using continuous broadband infrasound recordings. Today, the interpretation of these data motivates studies on passive remote sensing techniques to delineate the vertical structure of the stratospheric and mesospheric-thermospheric wind and temperature (e.g., Drob et al. 2010; Lalande et al. 2012; Assink et al. 2013; Assink et al. 2019). For example, the analysis of near-continuous infrasound detections of active volcanoes permits the evaluation of atmospheric products produced by ECMWF through the study of stratospheric propagation with a time resolution ranging from hours to multiple years (e.g., Assink et al. 2014). The global PMCC detection lists 2005–2010 produced by Matoza et al. (2013) were used for automated detection and cataloging of global explosive volcanism (Matoza et al. 2017, 2019), and the results from the present study can be used to extend these results to 2015. Comparison of regional volcano infrasound with simulations also allows the evaluation of middle atmospheric weather forecasts, providing new metrics to evaluate stratospheric skills (Smets et al. 2016).

With the increasing number of IMS stations (Marty 2019) complemented by dense regional networks at continental scales (e.g., de Groot-Hedlin and Hedlin 2019), systematic studies using historical infrasound datasets and state-of-the-art reanalysis systems provide useful integrated information about the structure of the stratosphere where data coverage is sparse (Lee et al. 2019). Of specific interest is the characterization of the four-dimensional stratopause evolution throughout the SSW life cycle and the study of the longer term influences of SSWs on the troposphere (e.g., Charlton-Perez et al. 2013; Smets and Evers 2014; Smets et al. 2019). It is expected that combining recent advances in modeling techniques, taking advantage of an infrastructure that integrates various independent middle atmospheric measurement techniques currently not assimilated in NWP models, would provide quantitative understanding of stratosphere–troposphere dynamical coupling useful for NWP applications (Blanc et al. 2019). Beyond the atmospheric community, the evaluation of NWP models is essential in the context of the future verification of the CTBT as improved atmospheric models are extremely helpful to assess the IMS network performance in higher resolution, reduce source location errors and characterization methods.

Acknowledgements We thank the CTBTO and station operators for guaranteeing the high quality of the infrasound data. This work was performed during the course of the ARISE design study (http://arise-project.eu), funded under the H2020 Framework Programme of the European Union (grant 653980).

References

Ardhuin F, Herbers THC (2013) Noise generation in the solid Earth, oceans and atmosphere, from nonlinear interacting surface, gravity waves infinite depth. J Fluid Mech 716:316–348. https://doi.org/10.1017/jfm.2012.548

Assink JD, Waxler R, Frazier WG, Lonzaga J (2013) The estimation of upper atmospheric wind model updates from infrasound data. J Geophys Res 118. https://doi.org/10.1002/jgrd.50833

Assink JD, Le Pichon A, Blanc E, Kallel M, Khemiri L (2014) Evaluation of wind and temperature profiles from ECMWF analysis on two hemispheres using volcanic infrasound. J Geophys Res Atmos 119. https://doi.org/10.1002/2014jd021632

Assink J, Smets P, Marcillo O, Weemstra C, Lalande J-M, Waxler R, Evers L (2019) Advances in infrasonic remote sensing methods. In: Le Pichon A, Blanc E, Hauchecorne A (eds) Infrasound monitoring for atmospheric studies, 2nd edn. Springer, Dordrecht, pp 605–632

Blanc E, Pol K, Le Pichon A, Hauchecorne A, Keckhut P, Baumgarten G, Hildebrand J, Höffner J, Stober G, Hibbins R, Espy P, Rapp M, Kaifler B, Ceranna L, Hupe P, Hagen J, Rüfenacht R, Kämpfer N, Smets P (2019) Middle atmosphere variability and model uncertainties as investigated in the framework of the ARISE project. In: Le Pichon A, Blanc E, Hauchecorne A (eds) Infrasound monitoring for atmospheric studies, 2nd edn. Springer, Dordrecht, pp 845–887

Brachet N, Brown D, Le Bras R, Mialle P, Coyne J (2010) Infrasound monitoring for atmospheric studies, chapter monitoring the earth's atmosphere with the global IMS infrasound network. Springer, Dordrecht, pp 77–118. ISBN:978-1-4020-9507-8

Campus P, Christie DR (2010) Infrasound monitoring for atmospheric studies. In: (eds) Le Pichon A, Blanc E, Hauchecorne A, chapter Worldwide observations of infrasonic waves. Springer, Dordrecht, pp 195–234. ISBN:978-1-4020-9507-8

Cansi Y (1995) An automatic seismic event processing for detection and location—the PMCC method. Geophys Res Lett 22:1021–1024

Charlton-Perez AJ et al (2013) On the lack of stratospheric dynamical variability in low-top versions of the CMIP5 models. J Geophys Res 118:2494–2505. https://doi.org/10.1002/jgrd.50125

Christie DR, Campus P (2010) Infrasound monitoring for atmospheric studies. In: Le Pichon A, Blanc E, Hauchecorne A (eds) Chapter the IMS infrasound network: design and establishment of infrasound stations. Springer, Dordrecht, pp 29–76. ISBN:978-1-4020-9507-8

Chunchuzov IP (1993) On the possible generation mechanism of non-stationary mountain waves in the atmosphere. J Atmos Sci 51:2196–2206

Chunchuzov I, Kulichkov S (2019) Internal gravity wave perturbations and their impacts on infrasound propagation in the atmosphere. In: Le Pichon A, Blanc E, Hauchecorne A (eds) Infrasound monitoring for atmospheric studies, 2nd edn. Springer, Dordrecht, pp 551–590

de Groot-Hedlin C, Hedlin M (2019) Detection of infrasound signals and sources using a dense seismic network. In: Le Pichon A, Blanc E, Hauchecorne A (eds) Infrasound monitoring for atmospheric studies, 2nd edn. Springer, Dordrecht, pp 669–699

Donn WL (1973) Sea wave origin of microbaroms and microseisms. J Geophys Res 78: 4482–4488

Drob D (2019) Meteorology, climatology, and upper atmospheric composition for infrasound propagation modeling. In: Le Pichon A, Blanc E, Hauchecorne A (eds) Infrasound monitoring for atmospheric studies, 2nd edn. Springer, Dordrecht, pp 485–508

Drob DP, Picone JM, Garcés M (2003) Global morphology of infrasound propagation. J Geophys Res 108:D21. https://doi.org/10.1029/2002JD003307

Drob DP, Meier RR, Picone JM, Garcés M (2010) Infrasound monitoring for atmospheric studies. In: Le Pichon A, Blanc E, Hauchecorne A (eds) chapter inversion of infrasound signals for passive atmospheric remote sensing, pp 701–731. Springer, Dordrecht. ISBN:978-1-4020-9507-8

Evers LG, Siegmund P (2009) The infrasonic signature of the 2009 major Sudden Stratospheric Warming. Geophys Res Lett 36:L23808. https://doi.org/10.1029/2009GL041323

Garcés M, Willis M, Hetzer C, Le Pichon A, Drob D (2004) On using ocean swells for continuous infrasonic measurements of winds and temperature in the lower, middle, and upper atmosphere. Geophys Res Lett 31. https://doi.org/10.1029/2004gl020696

Garcés MA (2013) On infrasound standard, part 1: time, frequency, and energy scaling, vol 2, pp 13–35. http://dx.doi.org/10.4236/inframatics.2013.22002

Green DN, Bowers D (2010) Estimating the detection capability of the International Monitoring System infrasound network. J Geophys Res 115:D18116. https://doi.org/10.1029/2010JD014017

Green DN, Le Pichon A, Ceranna L, Evers L (2010) Infrasound monitoring for atmospheric studies. In: Le Pichon A, Blanc E, Hauchecorne A, Chapter ground truth events: assessing the capability of infrasound networks using high resolution data analyses, Springer, Dordrecht, pp 599–625. ISBN:978-1-4020-9507-8

Green DN, Matoza RS, Vergoz J, Le Pichon A (2012) Infrasonic propagation from the 2010 Eyjafjallajökull eruption: investigating the influence of stratospheric solar tides. J Geophys Res 117:D21202. https://doi.org/10.1029/2012JD017988

Kim YJ, Arakawa A (1993) Improvement of orographic gravity waves parameterization using a mesoscale gravity wave model. J Atmos Sci 52:1902–1975

Lalande JM, Sèbe O, Landès M, Blanc-Benon P, Matoza RS, Le Pichon A, Blanc E (2012) Infrasound data inversion for atmospheric sounding. Geophys J Int 190. https://doi.org/10.1111/j.1365-246x.2012.05518.x

Landès M, Ceranna L, Le Pichon A, Matoza R (2012) Localization of microbarom sources using the IMS infrasound network. J Geophys Res. https://doi.org/10.1029/2011jd016684

Landès M, Le Pichon A, Shapiro N, Hillers G, Campillo M (2014) Explaining global patterns of microbarom observations with wave action models. Geophys J Int 2014(199):1328–1337. https://doi.org/10.1093/gji/ggu324

Larson RJ, Craine LB, Thomas JE, Wilson CR (1971) Correlation of winds and geographic features with production of certain infrasonic signals in the atmosphere. Geophys J R Astron Soc 26:201–214

Le Pichon A, Matoza R, Brachet N, Cansi Y (2010) Recent enhancements of the PMCC infrasound signal detector. Inframatics Newslett 26:5–8. http://www.inframatics.org

Le Pichon A, Ceranna L, Vergoz J (2012) Incorporating numerical modeling into estimates of the detection capability of the IMS infrasound network. J Geophys Res 117:D05121. https://doi.org/10.1029/2011JD016670

Le Pichon A, Assink JD, Heinrich P, Blanc E, Charlton-Perez A, Lee CF, Keckhut P, Hauchecorne A, Rüfenacht R, Kämpfer N et al (2015) Comparison of co-located independent ground-based middle-atmospheric wind and temperature measurements with Numerical Weather Prediction models. J Geophys Res 120. https://doi.org/10.1002/2015jd023273

Lee C, Smets P, Charlton-Perez A, Evers L, Harrison G, Marlton G (2019) The potential impact of upper stratospheric measurements on sub-seasonal forecasts in the extra-tropics. In: Le Pichon A, Blanc E, Hauchecorne A (eds) Infrasound monitoring for atmospheric studies, 2nd edn. Springer, Dordrecht, pp 889–910

Longuet-Higgins MS (1950) A theory of the origin of microseisms. R Soc Lond Phil Trans A 243:1–35

Marty J (2019) The IMS Infrasound network: current status and technological developments. In: Le Pichon A, Blanc E, Hauchecorne A (eds) Infrasound monitoring for atmospheric studies, 2nd edn. Springer, Dordrecht, pp 3–62

Matoza R, Landès M, Le Pichon A, Ceranna L, Brown D (2013) Coherent ambient infrasound recorded by the International Monitoring System. Geophys Res Lett 40. https://doi.org/10.1029/2012gl054329

Matoza RS, Green DN, Le Pichon A, Shearer PM, Fee D, Mialle P, Ceranna L (2017) Automated detection and cataloging of global explosive volcanism using the International Monitoring System infrasound network. J Geophys Res Solid Earth 122:2946–2971. https://doi.org/10.1002/2016JB013356

Matoza R, Fee D, Green D, Mialle P (2019) Volcano infrasound and the international monitoring system. In: Le Pichon A, Blanc E, Hauchecorne A (eds) Infrasound monitoring for atmospheric studies, 2nd edn. Springer, Dordrecht, pp 1023–1077

McFarlane MA (1987) The effect of orographically excited gravity waves drag on the general circulation of the lower stratosphere and troposphere. J Atmos Sci 44:1775–1800

Mialle P, Brown D, Arora N (2019) Advances in operational processing at the international data centre In: Le Pichon A, Blanc E, Hauchecorne A (eds) Infrasound monitoring for atmospheric studies, 2nd edn. Springer, Dordrecht, pp 209–248

Schimmel M, Stutzmann E, Ardhuin F, Gallart J (2011) Polarized Earth's ambient microseismic noise. Geochem Geophys Geosyst 12:Q07014. https://doi.org/10.1029/2011GC003661

Silber E, Brown P (2019) Infrasound monitoring as a tool to characterize impacting near-earth objects (NEOs). In: Le Pichon A, Blanc E, Hauchecorne A (eds) Infrasound monitoring for atmospheric studies, 2nd edn. Springer, Dordrecht, pp 939–986

Smets PSM, Evers LG (2014) The life cycle of a sudden stratospheric warming from infrasonic ambient noise observations. J Geophys Res 119. https://doi.org/10.1002/2014jd021905

Smets PSM, Assink JD, Le Pichon A, Evers LG (2016) ECMWF SSW forecast evaluation using infrasound. J Geophys Res Atmos 121. https://doi.org/10.1002/2015jd024251

Smets P, Assink J, Evers L (2019) The study of sudden stratospheric warmings using infrasound. In: Le Pichon A, Blanc E, Hauchecorne A (eds) Infrasound monitoring for atmospheric studies, 2nd edn. Springer, Dordrecht, pp 723–755

Smith RB, Woods K, Jensen J, Cooper WA, Doyle JD, Jiang Q, Grubisic V (2007) Mountain waves entering the stratosphere. J Atmos Sci 65. https://doi.org/10.1175/2007JAS2598.1

Stehly L, Campillo M, Shapiro NM (2006) A study of the noise from its long-range correlation properties. J Geophys Res 111:B10306. https://doi.org/10.1029/2005JB004237

Waxler R, Gilbert KE (2006) The radiation of atmospheric microbaroms by ocean waves. J Acoust Soc Am 119:2651–2664

Waxler R, Assink J (2019) Propagation modeling through realistic atmosphere and benchmarking. In: Le Pichon A, Blanc E, Hauchecorne A (eds) Infrasound monitoring for atmospheric studies, 2nd edn. Springer, Dordrecht, pp 509–549

Wilson CR, Szuberla CA, Olson JV (2010) Infrasound monitoring for atmospheric studies. In: Le Pichon A, Blanc E, Hauchecorne A (eds) Chapter high-latitude observations of infrasound from Alaska and Antarctica: mountains associated waves and geomagnetic/auroral infrasonic signals. Springer, Dordrecht, pp 415–451. ISBN:978-1-4020-9507-8